

Near-complete violation of Kirchhoff's law in thermal radiation in ultrathin magnetic Weyl semimetal films

Jun Wu¹, Zhongmin Wang², Han Zhai³, Zhangxing Shi³, Xiaohu Wu^{3,*}, and Feng
Wu^{4,*}

1. Key Laboratory of Advanced Perception and Intelligent Control of High-end Equipment,
Ministry of Education, College of Electrical Engineering, Anhui Polytechnic University,

Wuhu, 241000, China

2. Institute of Automation, Qilu University of Technology (Shandong Academy of Sciences),
Jinan 250014, China

3. Shandong Institute of Advanced Technology, Jinan 250100, China

4. School of Optoelectronic Engineering, Guangdong Polytechnic Normal University,

Guangzhou 510665, China

*Corresponding author: xiaohu.wu@iat.cn, fengwu@gpnu.edu.cn

Abstract: The ability to break Kirchhoff's law is of fundamental importance in thermal radiation. Various nonreciprocal emitters have been proposed to break the balance between absorption and emission. However, the thicknesses of the nonreciprocal materials are usually larger than 1/10 times of the wavelength. Besides, the previous proposed nonreciprocal emitters are complex, thus they can hardly be fabricated in experiment to verify the Kirchhoff's law for nonreciprocal materials. In this paper, we investigate the nonreciprocal thermal radiation of the magnetic Weyl semimetal (MWSM) film atop of the metal substrate. It is found that the strong nonreciprocal radiation at the wavelength of 9.15 μm can be achieved when the thickness of the MWSM film is 100 nm. The enhanced nonreciprocity is attributed to the Fabry-Perot resonances. The results indicate that the MWSM film is the promising candidate to engineer the ultrathin and simple nonreciprocal thermal emitters. What is perhaps most intriguing here is that the proposed structure can be more easily fabricated in experiment to verify the Kirchhoff's law for nonreciprocal materials.

Keywords: nonreciprocal thermal radiation, magnetic Weyl semimetal, Fabry-Perot resonances, Kirchhoff's law

1. Introduction

All objects at nonzero temperatures emit electromagnetic radiation according to the fundamental principle of statistical mechanics [1-4]. It has been long recognized in the literature that most thermal emitters obey the Kirchhoff's emission-absorption equivalence law. Therefore, the Kirchhoff's law plays a very significant role in understanding thermal emission. The recent emergence of nonreciprocal thermal emitters has opened new avenues for controlling fundamental aspects of thermal emission, because such emitters can break the Kirchhoff's law, i.e., breaking the balance between absorption and emission [5-23]. Since the traditional Kirchhoff's law is not applicable for nonreciprocal thermal emitters, the generalized Kirchhoff's law that is applicable for both reciprocal and nonreciprocal thermal emitters has been explored and derived [24-27].

Various nonreciprocal materials, including magneto-optical materials and magnetic Weyl semimetals (MWSMs), are engineered to break the equivalence between absorption and emission [11-23, 28]. Compared with magneto-optical materials, MWSMs possess intrinsic advantages, i.e., it has stronger nonreciprocity in the mid-infrared range without applying an external magnetic field [20-23]. Therefore, the MWSMs are the promising candidates for nonreciprocal thermal emitters. Besides, nonreciprocal thermal emitters containing magneto-optical materials usually need large thickness to enhance the difference between absorption and emission [11-17]. What is most important, complex structures are usually needed [11-17]. Although MWSMs possess intrinsic nonreciprocity, they have not been comprehensively

investigated to engineer nonreciprocal thermal emitters, especially for ultrathin and simple nonreciprocal thermal emitters. Grating structures and prism-coupling structures have been used to enhance the difference between absorption and emission of MWSMs [20, 23]. Due to the fabrication technologies, these structures are not easy to be fabricated in experiment at present. The fabrication of single MWSM film has been achieved by several groups [29-31]. However, the nonreciprocal thermal radiation of single MWSM film has not been fully explored.

In this work, the nonreciprocal radiation of a single MWSM film atop of the metal substrate is explored. The results show that strong nonreciprocal radiation at the wavelength of 9.15 μm can be achieved when the thickness of the MWSM film is 100 nm. The enhanced nonreciprocity is attributed to the Fabry-Perot (FP) resonances. Our results show that the MWSM film is the promising candidate to engineer the ultrathin and simple nonreciprocal thermal emitters. Besides, the structure is promising to be used to verify the Kirchhoff's law for nonreciprocal materials, since it can be easily fabricated in experiment [31].

2. Model

In this work, the proposed structure is shown in Fig. 1, where a MWSM film with a thickness of d_1 is on the top of the silver (Ag) substrate. The relative permittivity of Ag is described by the Drude model, i.e., $\varepsilon_{\text{Ag}} = \varepsilon_{\infty} - \omega_p^2 / (\omega^2 + j\omega\Gamma)$, with $\varepsilon_{\infty} = 3.4$, $\omega_p = 1.39 \times 10^{16}$ rad/s, $\Gamma = 2.7 \times 10^{13}$ rad/s, and ω is the angular frequency [32]. The wavevector component along the x -axis is $k_x = k_0 \sin \theta$, where k_0 is the wavevector in the vacuum and θ is the angle of incidence.

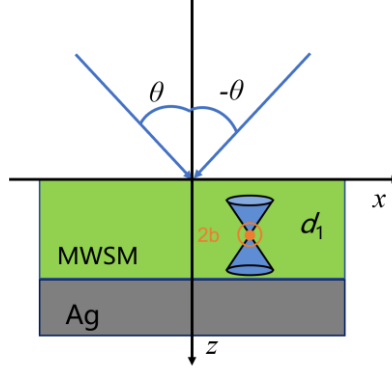


Fig. 1 Schematic of the proposed nonreciprocal thermal emitters. The MWSM film with a thickness of d_1 is on the top of the metal substrate.

When each pair of Weyl nodes are separated along the y -axis in the momentum space, the relative permittivity tensor of the MWSM can be described as [20, 23]

$$\boldsymbol{\varepsilon} = \begin{bmatrix} \varepsilon_d & 0 & -j\varepsilon_a \\ 0 & \varepsilon_d & 0 \\ j\varepsilon_a & 0 & \varepsilon_d \end{bmatrix}. \quad (1)$$

The detail expressions of the relative permittivity components can be found in Refs. [21] and [24]. When ε_a is zero, the permittivity tensor is symmetric, thus obeying Lorentz reciprocity [35]. When ε_a is nonzero, the permittivity tensor is asymmetric, thus breaking Lorentz reciprocity [35]. When the temperature is 300 K, two components ε_d and ε_a are shown in Fig. 2. ε_d is a complex number while ε_a is a real number. One can see that the epsilon-near-zero wavelength is about 8.6 μm . The real part $\text{Re}(\varepsilon_d)$ is negative when the wavelength is larger than 8.6 μm . The ε_a increases with the wavelength, indicating that stronger nonreciprocity can be achieved at larger wavelengths.

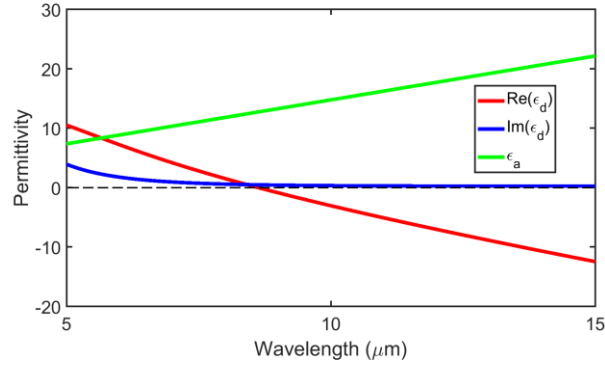


Fig. 2 Relative permittivity of the MWSM as a function of the wavelength. Black dashed line represents zero permittivity.

The plane of incidence is x - z plane, thus there is no polarization conversion between two linearly polarized waves. When a TM- (transverse magnetic, with the magnetic field along the direction of y -axis) polarized plane wave is incident with an angle θ , the spectral directional absorption and emission of the structure can be calculated by [26]

$$\alpha(\theta, \lambda) = 1 - R(\theta, \lambda), e(\theta, \lambda) = 1 - R(-\theta, \lambda). \quad (2)$$

Here, $R(\theta, \lambda)$ and $R(-\theta, \lambda)$ are the reflection for the incident angle of θ and $-\theta$ at the wavelength λ , respectively. The difference between emission and absorption is defined as $\eta = |\alpha - e|$, which measuring the nonreciprocal radiation. The transfer matrix method for calculating the reflection of the multilayer structures with nonreciprocal materials is presented in Ref. [17].

3. Results and discussion

The difference between the absorption and emission varying with the angle of incidence and wavelength for different thicknesses of the MWSM film d_1 are shown

in Fig. 3. When the thickness is equal to or larger than $10\ \mu\text{m}$, the ultra-strong nonreciprocal radiation is located around the wavelength of $8.3\ \mu\text{m}$ and the angle of incidence is 89° . When the thickness is $1\ \mu\text{m}$, besides the wavelength of $8.3\ \mu\text{m}$, large difference between absorption and emission can take place at the wavelength around $10.6\ \mu\text{m}$, as shown in Fig. 3(d). When the thickness is equal to or smaller than $0.1\ \mu\text{m}$, as shown in Figs. 3(e) and 3(f), the absorption and emission are almost identical at the wavelength of $8.3\ \mu\text{m}$. When the thickness is $0.1\ \mu\text{m}$, the strong nonreciprocal radiation is around the wavelength of $9.15\ \mu\text{m}$. When the thickness is $0.01\ \mu\text{m}$, the nonreciprocal radiation is quite weak for all the wavelengths and the angle of incidence. To sum up, the thickness of the MWSM film has a great impact on the nonreciprocal radiation.

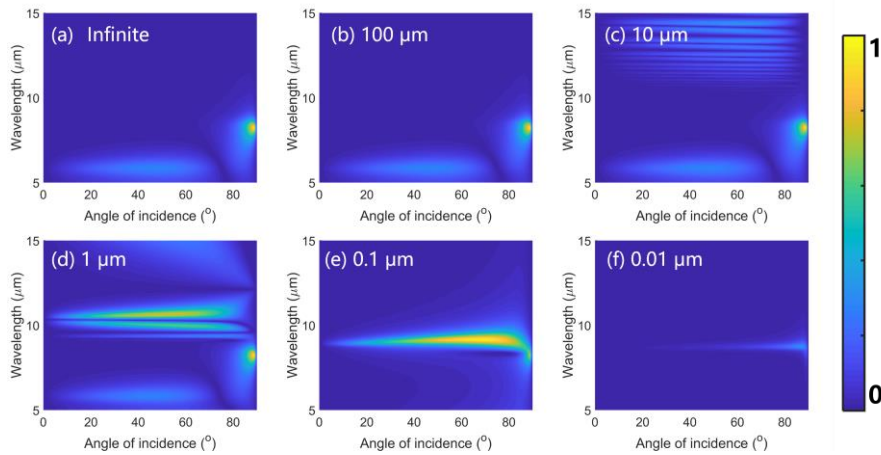


Fig. 3 Difference between the absorption and emission varying with the angle of incidence and the wavelength with difference thicknesses of the MWSM film d_1 : (a) infinite, (b) $100\ \mu\text{m}$, (c) $10\ \mu\text{m}$, (d) $1\ \mu\text{m}$, (e) $0.1\ \mu\text{m}$, and (f) $0.01\ \mu\text{m}$.

When the thickness of the MWSM film is $10\ \mu\text{m}$ and the angle of incidence is 89° , the absorption and emission are respectively shown in Fig. 4(a). One can see that the difference between the absorption and emission can reach 0.9 at the wavelength of

8.3 μm , indicating the near-complete violation of the Kirchhoff's law. The absorption and emission are almost the same when the wavelength is larger than 11 μm . In addition, the absorption and emission oscillate with the wavelength, indicating that FP resonances occur at larger wavelengths. Fig. 4(b) shows the absorption and emission varying with the thickness of the MWSM film at the wavelength of 8.3 μm when the angle of incidence is 89° . The absorption and emission do not change with the thickness when the thickness is larger than 0.4 μm , which indicates that the difference between them is stable. The absorption gets its maximum at $d_1=73$ nm with a smooth peak. The emission gets its maximum at $d_1=27$ nm with a sharper peak. These two peaks are attributed to the FP resonances. Only first order of FP resonance can be supported, either for the absorption or the emission. Such phenomenon has been observed and explained in a single hyperbolic material film [36]. To confirm that, one can analyze the wavevector in the MWSM film. The wavevector component along the z -axis in the MWSM film can be calculated by $k_{z1} = \sqrt{\varepsilon_v k_0^2 - k_x^2}$, where the effective relative permittivity is $\varepsilon_v = \varepsilon_d - \varepsilon_a^2 / \varepsilon_d$. At the wavelength of 8.3 μm , we have $\varepsilon_d = 0.79 + 0.54j$ and $\varepsilon_a = 12.27$. Therefore, we have $k_{z1} = (3.72 + 11.95j)k_0$. The imaginary part of k_{z1} is so large that the wave decays very fast during propagation in the film. Hence, the higher-order FP resonances cannot be supported. When the thickness of MWSM film is 10 μm , the distribution of magnetic field at the wavelength of 8.3 μm along the y -axis is plotted in Fig. 4(c). One can see that the field is strongly located at the interface between the air and the MWSM film. The field is stronger at angle of incidence of 89° than that at angle of incidence of -89° .

The stronger is the field, the smaller is the reflection. Therefore, the absorption is larger than the emission.

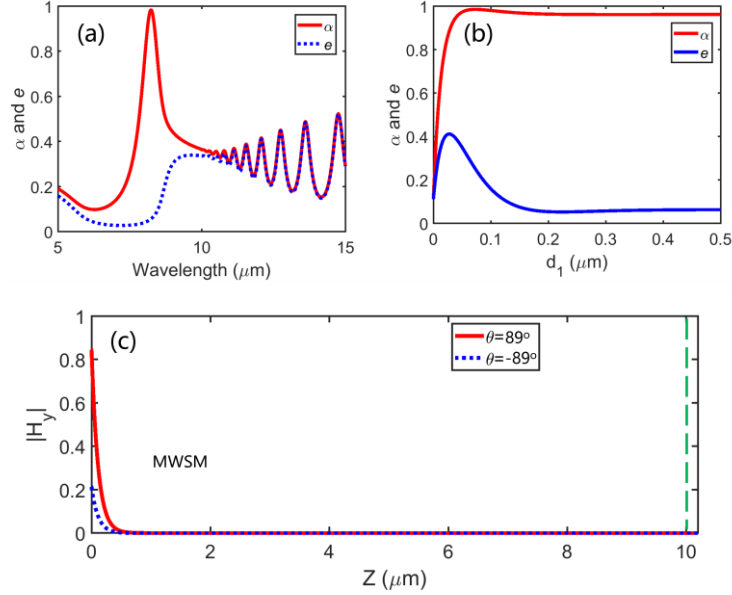


Fig. 4 (a) Absorption and emission spectra when the thickness of the MWSM film is 10 μm and the angle of incidence is 89° . (b) Absorption and emission as a function of the thickness of the MWSM film when the wavelength is 8.3 μm and the angle of incidence is 89° . (c) Distributions of the magnetic field at the wavelength of 8.3 μm at angles of incidence of 89° and -89° when the thickness of the MWSM film is 10 μm .

According to the permittivity of MWSM in Fig. 2, the wavelength of 8.3 μm is not a special point. However, the nonreciprocity at this wavelength is much larger than other wavelengths. To understand this, the reflection as functions of the angle of incidence and the wavelength is shown in Fig. 5. The thickness is infinite. Under this situation, the reflection is only related to the permittivity of the MWSM and the angle of incidence. It is clear the reflection is strong in the wavelength range between 6.5 μm and 9 μm , regardless of the sign of the angle of incidence. At the wavelength of 8.3 μm , the reflection is very small at angle of 89° , while it is large at angle of -89° .

Therefore, the nonreciprocity is strongly related with the permittivity at different wavelengths.

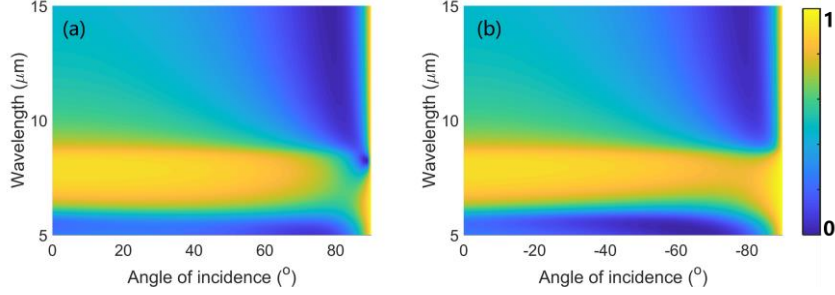


Fig. 5 Reflection as functions of the angle of incidence and the wavelength when the thickness of the MWSM film is infinite: (a) positive angle of incidence and (b) negative angle of incidence.

If ε_a is zero, the reflection should be high when the wavelength is larger than $8.6 \mu\text{m}$ since $\text{Re}(\varepsilon_d)$ is negative. However, if ε_a is not zero, the situation is quite different. As shown in Fig. 5, the reflection is small when the wavelength is larger than $9 \mu\text{m}$. To understand this point, it is necessary to analyze the value of the effective relative permittivity $\varepsilon_v = \varepsilon_d - \varepsilon_a^2 / \varepsilon_d$ since it impacts the wavevector in the MWSM film. The real and imaginary parts of $\varepsilon_v = \varepsilon_d - \varepsilon_a^2 / \varepsilon_d$ are shown in Fig. 6. One can see that the real part of ε_v is negative in the band between $5.7 \mu\text{m}$ and $8.6 \mu\text{m}$. Besides, the peak of the imaginary part is located around $8.65 \mu\text{m}$, and its maximum is much larger than $\text{Im}(\varepsilon_d)$ shown in Fig. 2. The negative real part of ε_v leads to high reflection. Therefore, the high reflection in Fig. 5 can be understood by looking at the value of ε_v .

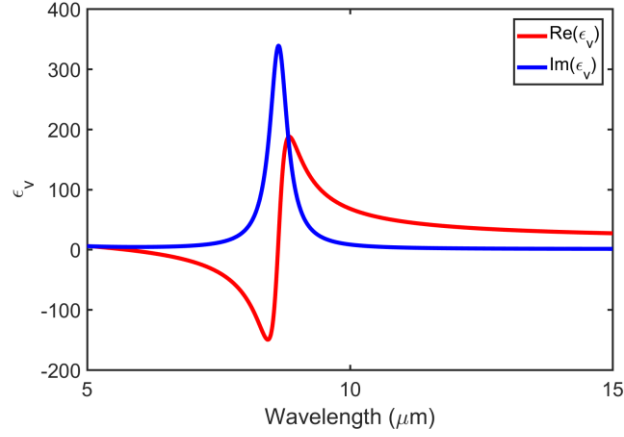


Fig. 6 Real and imaginary parts of ϵ_v as a function of the wavelength.

When the thickness of the MWSM film is $0.1 \mu\text{m}$ and the angle of incidence is 68° , the absorption and emission are shown in Fig. 7(a). The absorption can reach 0.995 at the wavelength of $9.15 \mu\text{m}$, while the emission is smaller than 0.03. The difference between them is higher than 0.96. Fig. 7(b) shows the absorption and emission varying with the thickness of the MWSM film. It is clear that both of them oscillate with the wavelength, indicating that FP resonances occur. The distance between adjacent peaks in the absorption spectra is about $0.39 \mu\text{m}$, and that is also about $0.39 \mu\text{m}$ in the emission spectra. It is reasonable because the wavevectors in the MWSM film are the same, regardless of the sign of the angle of incidence. To check the excitation of FP resonances, the distance between two adjacent peaks should satisfy [36]

$$\text{Re}(k_{z1})\Delta = \pi, \quad (3)$$

where Δ is the distance between two adjacent FP resonances. At the wavelength of $9.15 \mu\text{m}$, there is $\epsilon_d = -1.19 + 0.42j$, $\epsilon_a = 13.52$, $k_{z1} = (11.80 + 2.05j)k_0$. According to Eq. (3), the calculated distance between two FP resonances should be $0.388 \mu\text{m}$, which is very close to $0.39 \mu\text{m}$. Therefore, Eq. (3) can confirm the

excitation of FP resonances.

Besides, it is noted that the absorption reaches its maximum when the thickness is $0.1 \mu\text{m}$. Therefore, the strong nonreciprocal radiation shown in Fig. 7(a) is attributed to the excitation of FP resonances in the MWSM film. The distribution of magnetic field at the wavelength of $9.15 \mu\text{m}$ along the z -axis is plotted in Fig. 7(b). The intensity of the incident magnetic field is set to be unity. When the angle of incidence is 68° , the magnetic field is enhanced at the interface between the MWSM film and the Ag substrate, thus the absorption is large in this case. However, the magnetic field is smaller at the interface for angle of incidence of -68° , indicating that most of the incidence wave is reflected. According to Eq. (2), the emission is small for angle of incidence of 68° .

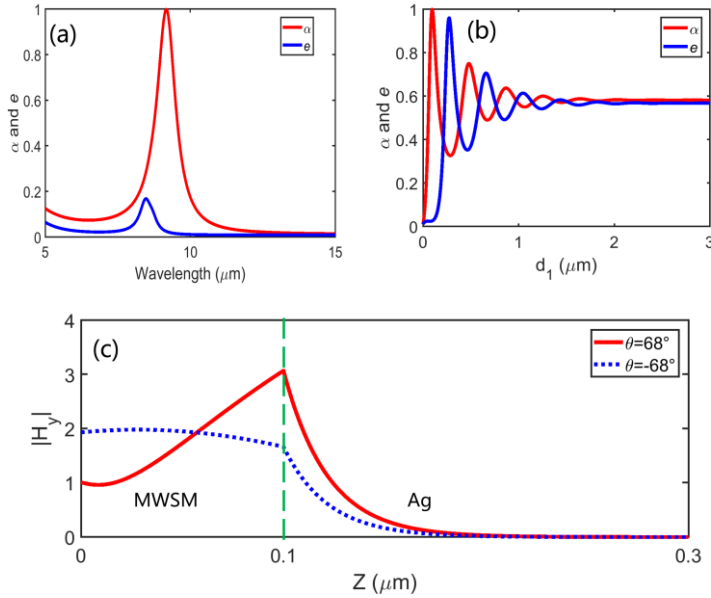


Fig. 7 (a) Absorption and emission spectra when the thickness of the MWSM film is $0.1 \mu\text{m}$ and the angle of incidence is 68° . (b) Absorption and emission as a function of the thickness of the MWSM film when the wavelength is $9.15 \mu\text{m}$ and the angle of incidence is 68° . (c) Distributions of the magnetic field at the wavelength of $9.15 \mu\text{m}$ at angles of incidence of 68° and -68° when the

thickness of the MWSM film is $0.1 \mu\text{m}$.

At the wavelength of $9.15 \mu\text{m}$, the absorption, emission, and the difference between them as functions of the angle of incidence and the thickness of the MWSM is shown in Fig. 8. According to Figs. 8(a) and 8(b), one can see that the first order FP resonance is strong, while the other orders are weak. Besides, strong absorption and emission are realized at large angle of incidence. As shown in Fig. 8(c), it is clear the nonreciprocal radiation is strong at the first order FP resonance. In addition, the large difference between absorption and emission can be realized when the angle of incidence is larger than 40° . It is hard to realize strong nonreciprocal radiation at small angles of incidence.

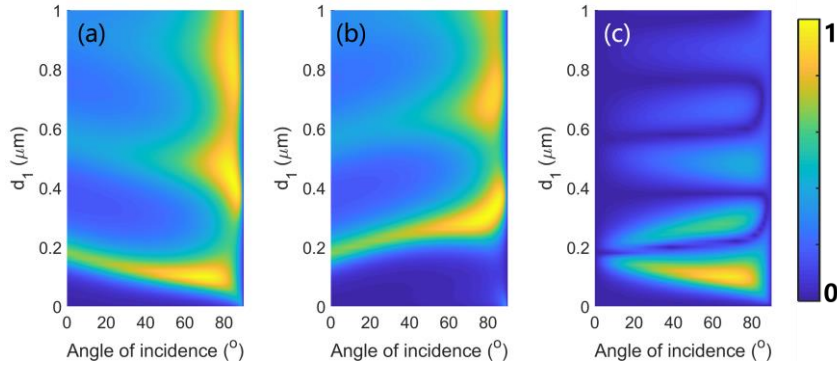


Fig. 8 (a) Absorption, (b) emission, and (c) the difference between them varying with the angle of incidence and the thickness of the MWSM at the wavelength of $9.15 \mu\text{m}$.

4. Conclusions

In summary, the nonreciprocal thermal radiation based on MWSM film is investigated. The transfer matrix method is used to calculate the absorption and emission. The results show that strong nonreciprocal radiation at the wavelength of $9.15 \mu\text{m}$ can be achieved when the thickness of the MWSM film is 100 nm . The

enhanced nonreciprocity is attributed to the FP resonances. Our results can not only deepen our understanding about the nonreciprocity of the MWSM films, but also show that the MWSM film is the promising candidate to engineer the ultrathin and simple nonreciprocal thermal emitters.

Acknowledgements

The authors acknowledge the support of the National Natural Science Foundation of China (Grant Nos. 61405217, 52106099 and 12104105), the Zhejiang Provincial Natural Science Foundation (Grant No. LY20F050001), the Anhui Provincial Natural Science Foundation (Grant No. 2108085MF231), the Anhui Polytechnic University Research Startup Foundation (Grant No. 2020YQQ042), the Pre-research Project of National Natural Science Foundation of Anhui Polytechnic University (Grant No. Xjky02202003), the Natural Science Foundation of Shandong Province (Grant No. ZR2020LLZ004), and the Start-Up Funding of Guangdong Polytechnic Normal University (Grant No. 2021SDKYA033).

References

1. D. G. Baranov, Y. Xiao, I. A. Nechepurenko, A. Krasnok, A. Alu, and M. A. Kats, Nanophotonic engineering of far-field thermal emitters, *Nat. Mater.* 18, 920-930 (2019).
2. Y. Li, W. Li, T. Han, X. Zheng, J. Li, B. Li, S. Fan, and C. W. Qiu, Transforming heat transfer with thermal metamaterials and devices, *Nat. Rev. Mater.* 6, 1-20 (2021).
3. W. Li, and S. Fan, Nanophotonic control of thermal radiation for energy

- applications, *Opt. Express* 26, 15995-16021 (2018).
4. X. H. Wu, *Thermal radiative properties of uniaxial anisotropic materials and their manipulations*, Singapore: Springer; 2021.
 5. L. Zhu, and S. Fan, Persistent directional current at equilibrium in nonreciprocal many-body near field electromagnetic heat transfer, *Phys. Rev. Lett.* 117, 134303 (2016).
 6. J. Dong, W. J. Zhang, and L. H. Liu, Nonreciprocal thermal radiation of nanoparticles via spin-directional coupling with reciprocal surface modes, *Appl. Phys. Lett.* 119, 021104 (2021).
 7. J. Dong, W. Zhang, and L. Liu, Electromagnetic scattering, absorption and thermal emission by clusters of randomly distributed magneto-optical nanoparticles, *J. Quant. Spectrosc. Radiat. Transfer* 255, 107279 (2020).
 8. L. J. Fernandez-Alcazar, R. Kononchuk, H. Li, and T. Kottos, Extreme nonreciprocal near-field thermal radiation via Floquet photonics, *Phys. Rev. Lett.* 126, 204101 (2021).
 9. L. Remer, E. Mohler, W. Grill, and B. Luthi, Nonreciprocity in the optical reflection of magnetoplasmas, *Phys. Rev. B* 30, 3277-3282 (1984).
 10. W. C. Snyder, Z. Wan, and X. Li, Thermodynamic constraints on reflectance reciprocity and Kirchhoff's law, *Appl. Opt.* 37, 3464-3470 (1998).
 11. L. Zhu, and S. H. Fan, Near-complete violation of detailed balance in thermal radiation, *Phys. Rev. B* 90, 220301 (2014).
 12. B. Zhao, Y. Shi, J. Wang, Z. Zhao, N. Zhao, and S. Fan, Near-complete violation

- of Kirchhoff's law of thermal radiation with a 0.3 T magnetic field, *Opt. Lett.* 44, 4203-4206 (2019).
13. X. H. Wu, The Promising Structure to Verify the Kirchhoff's Law for Nonreciprocal Materials, *ES Energy Environ.* 12, 46-51 (2021).
 14. X. H. Wu, Z. X. Chen, and F. Wu, Strong Nonreciprocal Radiation in a InAs Film by Critical Coupling with a Dielectric Grating, *ES Energy Environ.* 13, 8-12 (2021).
 15. X. H. Wu, R. Y. Liu, H. Y. Yu, and B. Y. Wu, Strong nonreciprocal radiation in magnetophotonic crystals, *J. Quant. Spectrosc. Radiat. Transfer* 272, 107794 (2021).
 16. J. Wu, F. Wu, and X. H. Wu, Strong dual-band nonreciprocal radiation based on a four-part periodic metal grating, *Opt. Mater.* 120, 111476 (2021).
 17. J. Wu, F. Wu, T. Zhao, M. Antezza, and X. H. Wu, Dual-band nonreciprocal thermal radiation by coupling optical Tamm states in magnetophotonic multilayers, arXiv:2109.01969.
 18. A. Caratenuto, F. Chen, Y. Tian, M. Antezza, G. Xiao, and Y. Zheng, Magnetic field-induced emissivity tuning of InSb-based metamaterials in the terahertz frequency regime, *Opt. Mat. Express* 11, 3141-3153 (2021).
 19. M. He, H. Qi, Y. X. Su, Y. Ren, Y. Zhao, and M. Antezza, Giant thermal magnetoresistance driven by graphene magnetoplasmon, *Appl. Phys. Lett.* 117, 113104 (2020).
 20. B. Zhao, C. Guo, C. A. A. Garcia, P. Narang, and S. H. Fan, Axion-Field-Enabled

- Nonreciprocal Thermal Radiation in Weyl Semimetals, *Nano Lett.* 20, 1923-1927, (2020).
21. S. Pajovic, Y. Tsurimaki, X. Qian, and G. Chen, Intrinsic nonreciprocal reflection and violation of Kirchhoff's law of radiation in planar type-I magnetic Weyl semimetal surfaces, *Phys. Rev. B* 102, 165417 (2020).
 22. Y. Tsurimaki, X. Qian, S. Pajovic, F. Han, M. Li, and G. Chen, Large nonreciprocal absorption and emission of radiation in type-I Weyl semimetals with time reversal symmetry breaking, *Phys. Rev. B* 101, 165426 (2020).
 23. X. H. Wu, H. Yu, F. Wu, and B. Wu, Enhanced nonreciprocal radiation in Weyl semimetals by attenuated total reflection, *AIP Adv.* 11, 075106 (2021).
 24. Y. Hadad, J. C. Soric, and A. Alu, Breaking temporal symmetries for emission and absorption, *Proc. Natl. Acad. Sci.* 113, 3471-3475 (2016).
 25. D. A. B. Miller, L. Zhu, and S. Fan, Universal modal radiation laws for all thermal emitters, *Proc. Natl. Acad. Sci.* 114, 4336-4341 (2017).
 26. Z. M. Zhang, X. H. Wu, and C. J. Fu, Validity of Kirchhoff's law for semitransparent films made of anisotropic materials, *J. Quant. Spectrosc. Radiat. Transfer* 245, 106904 (2020).
 27. C. Khandekar, F. Khosravi, Z. Li, and Z. Jacob, New spin-resolved thermal radiation laws for nonreciprocal bianisotropic media, *New J. Phys.* 22, 123005 (2020).
 28. T. A. Morgado and M. G. Silveirinha, Nonlocal effects and enhanced nonreciprocity in current-driven graphene systems, *Phys. Rev. B* 102, 075102

- (2020).
29. N. Morali, R. Batabyal, P. K. Nag, E. Liu, Q. Xu, Y. Sun, B. Yan, C. Felser, N. Avraham, and H. Beidenkopf, Fermi-arc diversity on surface terminations of the magnetic Weyl semimetal $\text{Co}_3\text{Sn}_2\text{S}_2$, *Science* 365, 1286-1291 (2019).
 30. Q. Wang, Y. Xu, R. Lou, Z. Liu, M. Li, Y. Huang, D. Shen, H. Weng, S. Wang, and H. Lei, Large intrinsic anomalous Hall effect in half-metallic ferromagnet $\text{Co}_3\text{Sn}_2\text{S}_2$ with magnetic Weyl fermions, *Nat. Commun.* 9, 3681 (2018).
 31. Q. Wang, Y. Zeng, K. Yuan, Q. Zeng, P. Gu, X. Xu, H. Wang, Z. Han, K. Nomura, W. Wang, E. Liu, Y. Hou, and Y. Ye, High-efficiency magnetism modulation of a single $\text{Co}_3\text{Sn}_2\text{S}_2$ layer directly by current, arXiv: 2011.08391 (2020).
 32. X. H. Wu, and C. J. Fu, Unidirectional transmission based on polarization conversion and excitation of magnetic or surface polaritons, *AIP Adv.* 7, 075208 (2017).
 33. R. Macedo, T. Dumelow, R. E. Camley, and R. L. Stamps, Oriented asymmetric wave propagation and refraction bending in hyperbolic media, *ACS Photon.* 5, 5086-5094 (2018).
 34. R. Macedo, and R. E. Camley, Engineering terahertz surface magnon-polaritons in hyperbolic antiferromagnets, *Phys. Rev. B* 99, 014437 (2019).
 35. S. Pajovic, Y. Tsurimaki, X. Qian, and S. V. Boriskina, Radiative heat and momentum transfer from materials with broken symmetries: opinion, *Opt. Mater. Express* 11, 3125-3131 (2021).
 36. X. H. Wu and C. J. Fu, Manipulation of enhanced absorption with tilted hexagonal boron nitride slabs, *J. Quant. Spectrosc. Radiat. Transfer* 209, 150-155 (2018).